AMERICAN SOCIETY FOR MICROBIOLOGY | mSphere

Check for updates

| Editor's Pick | Computational Biology | Research Article

Defining neuronal responses to the neurotropic parasite *Toxoplasma gondii*

Hannah J. Johnson,[1,2] Joshua A. Kochanowsky,[2,3] Sambamurthy Chandrasekaran,[2] Christopher A. Hunter,[4] Daniel P. Beiting,[4] Anita A. Koshy[1,2,3,5]

AUTHOR AFFILIATIONS See affiliation list on p. 10.

ABSTRACT A select group of pathogens infects neurons in the brain. Prior dogma held that neurons were "defenseless" against infecting microbes, but many studies suggest that neurons can mount anti-microbial defenses. However, a knowledge gap in understanding how neurons respond *in vitro* and *in vivo* to different classes of microorganisms remains. To address this gap, we compared a transcriptional data set derived from primary neuron cultures (PNCs) infected with the neurotropic intracellular parasite *Toxoplasma gondii* with a data set derived from neurons injected with *T. gondii* protein *in vivo*. These curated responses were then compared to the transcriptional responses of PNCs infected with the single-stranded RNA viruses, West Nile virus or Zika virus. These analyses highlighted a conserved response to infection associated with chemokines (*Cxcl10, Ccl2*) and cytokines (interferon signaling). However, *T. gondii* had diminished IFN-α signaling *in vitro* compared to the viral data sets and was uniquely associated with a decrease in neuron-specific genes (*Snap25*, *Slc17a7*, *Prkcg*). These data underscore that neurons participate in infection-induced neuroinflammation and illustrate that neurons possess both pathogen-specific and pathogen-conserved responses.

IMPORTANCE Though neurons are commonly the target of pathogens that infect the central nervous system (CNS), few data sets assess the neuronal response to infection. This paucity of data is likely because neurons are perceived to have diminished immune capabilities. However, to understand the role of neurons in neuroinflammation and their immune capabilities, their responses must be investigated. Here, we analyzed publicly accessible, neuron-specific data sets to compare neuron responses to a eukaryotic pathogen vs two Orthoflaviviruses. A better understanding of neuron responses to different infections will allow us to develop methods for inhibiting pathways that lead to neuron dysfunction, enhancing those that limit pathogen survival, and mitigating infection-induced damage to the CNS.

KEYWORDS *Toxoplasma gondii*, *T. gondii*, neurons, RNA-seq, transcriptomics, host response, central nervous system infections

A select number of microbes (e.g., measles virus and *Toxoplasma gondii*) infect the central nervous system (CNS). For many of these infections, neurons are the CNS cell that is primarily infected (1–3). Until relatively recently, dogma suggested this neuronal predominance arose from neurons lacking cell-intrinsic immune responses. Over several decades, work focusing on viral-neuron interactions established that neurons have cell-intrinsic responses, though these responses can differ from other cell types and even between neuron subtypes (4–7). These studies raise the question of whether the cellular immunity of neurons varies by context and/or pathogen. The eukaryotic intracellular parasite *Toxoplasma gondii* is a non-viral microbe with a tropism for neurons (8) and a broad natural host range, including rodents and humans (9). During infection,

Editor Ira J. Blader, Virginia-Maryland College of Veterinary Medicine, Blacksburg, Virginia, USA

Address correspondence to Daniel P. Beiting, beiting@vet.upenn.edu, or Anita A. Koshy, akoshy@arizona.edu.

The authors declare no conflict of interest.

See the funding table on p. 10.

Received 28 March 2025
Accepted 30 April 2025
Published 30 May 2025

parasites invade the CNS where they can infect multiple cell types, but in neurons, a portion of parasites switch to a slow-growing stage that forms tissue cysts (1, 10, 11). These tissue cysts cause a persistent, asymptomatic infection, potentially for the lifetime of the host (10–12). Recent studies suggest that the immune system can recognize infected neurons, contributing to local control of *T. gondii in vivo* (13–16). *In vitro* studies have shown that neurons can be activated by IFN-γ to limit parasite growth (17). Like most intracellular microbes, all of which depend upon the host cell for survival, *T. gondii* highly manipulates its host cell through the secretion of effector proteins. Most of the studies that define how these effector proteins manipulate cells were done *in vitro* in fibroblasts and immune cells such as macrophages (18, 19). While such studies have revealed fundamental aspects of *T. gondii*-host cell biology, they will have missed neuron-specific effects or effects only triggered during *in vivo* infection. The importance of understanding these nuances is highlighted by studies showing that outcomes of *T. gondii*-host cell interactions can vary by *T. gondii* strain and host cell (20–23).

We previously tried to address this gap by using laser capture microdissection (LCM) in combination with our *T. gondii*-Cre system (24). In this system, we use parasites that express a *T. gondii*::Cre recombinase fusion protein (ROP::Cre) to infect Cre reporter mice that express a green fluorescent protein (GFP) only after Cre-mediated recombination. Because the ROP::Cre protein is introduced into the host cell concomitantly with other early effectors (ROPs) and before full invasion, neurons injected with the ROPs will express GFP even if they cleared the parasite or were never invaded (i.e., aborted invasion) (25–27). We then used LCM and RNA-seq to isolate, pool, and transcriptionally profile the somas of *T. gondii*-injected (GFP^+) neurons (TINs). Though a small area centered on TINs' somas was captured, these transcriptional data still contained immune cell transcripts (24), making it difficult to distinguish which differentially expressed genes (DEGs) or pathways were derived from neurons, immune cells, or both.

In this study, we sought to identify neuron-specific responses to *T. gondii* by comparing RNA-seq data sets from our *in vivo* data with a newly generated *in vitro* data set from *T. gondii*-infected primary neuron cultures (PNCs). This analysis revealed a set of conserved pathways driven by chemokines, such as *Ccl2* and *Cxcl10*. The comparison to previously published transcriptomes of West Nile virus (WNV)-infected and Zika virus (ZKV)-infected PNCs (7) revealed pathways that were conserved between these data sets and others that were pathogen dependent. For example, *T. gondii* data sets revealed a decrease in neuron-specific genes (e.g., *Snap25*, *Slc17a7*, and *Prkcg*) that were unchanged in virally infected neurons. Conversely, the type I IFN (IFN-α) response pathway was upregulated by WNV and ZKV and, to some extent, by *T. gondii in vivo* but not by *T. gondii in vitro*. In summary, the ability to compare the *in vitro* and *in vivo* response of neurons to infection highlights that neurons have intrinsic, microbe-specific responses that are modulated *in vivo*.

RESULTS

Conserved neuron response genes and pathways in *T. gondii* infection models

Transcriptomic data from neurons in two *T. gondii* infection conditions—neurons in tissue sections isolated with laser capture microdissection (24) and cortical primary neuron cultures (Fig. 1)—were compared to find common neuron response pathways. Briefly, in a previous report, we combined transgenic parasites that secrete Cre recombinase with a mouse strain that expresses a Cre-sensitive GFP reporter, which allowed us to isolate *T. gondii*-injected neurons (GFP^+NeuN^+) by LCM (27). The RNA from these neurons was isolated, sequenced, and compared with neurons from uninfected mice (Fig. 1A).

In a separate study, PNCs infected with *T. gondii* for 24 hours were used to assess how infection altered the neuronal transcriptome. Reads were filtered, normalized, and represented as counts per million, shown in Fig. S1A through C. As expected, principal component analysis of the LCM and PNC data sets revealed marked differences between infected and uninfected controls (Fig. S1D and E), with over 2,100 differentially expressed

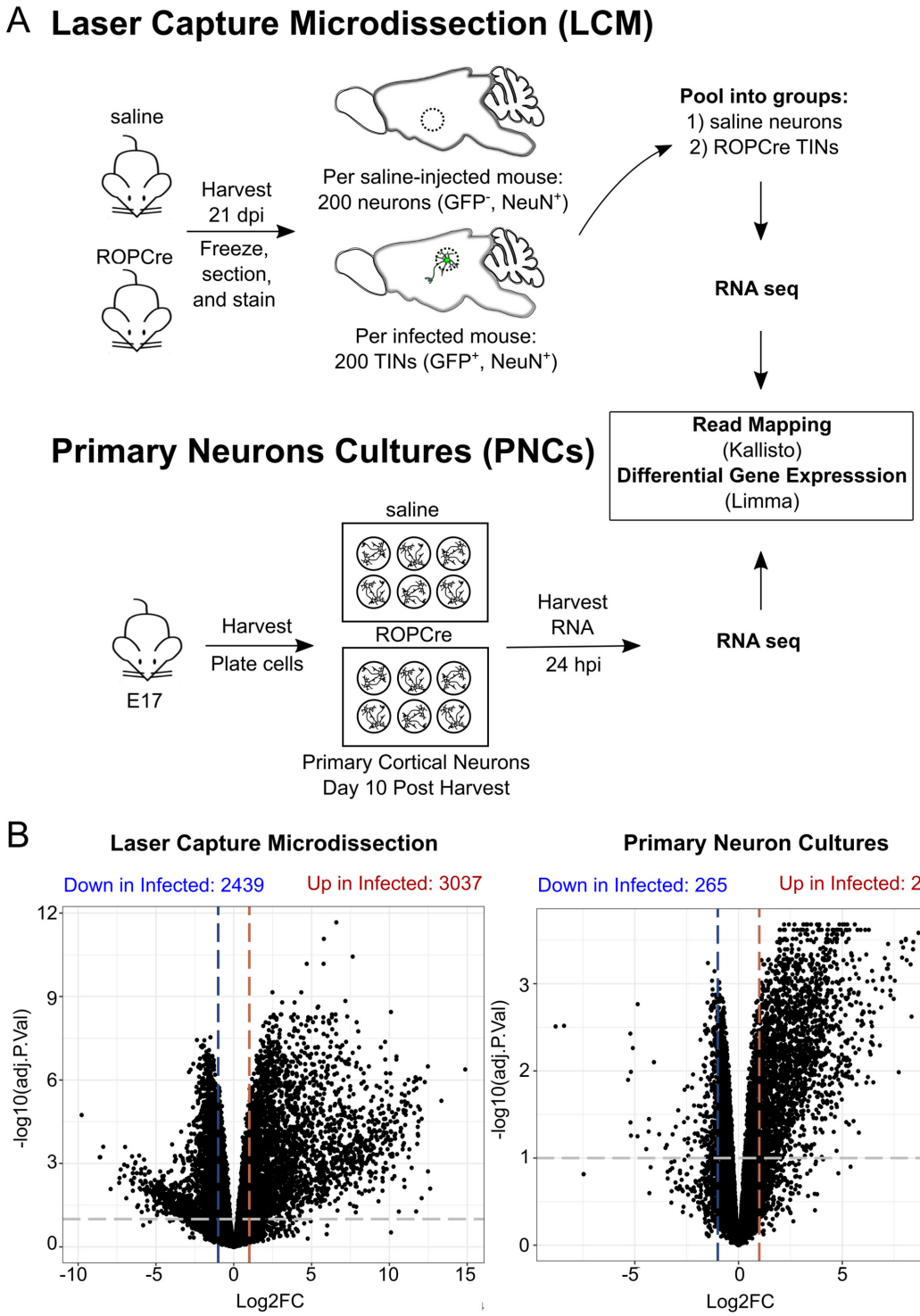

FIG 1 *T. gondii*-infected neurons from *in vitro* (PNC) and *in vivo* (LCM) systems were captured and analyzed for differentially expressed genes. (A) Experimental schematic of neurons captured by laser capture microdissection and infected primary murine neuronal cultures. (B) Volcano plots of differentially expressed genes in both data sets. Horizontal bars indicate adjusted *P* values ≤0.1, and vertical bars indicate $\log_2$ fold change ≥1 for up- and downregulated genes.

genes compared to uninfected controls (false discovery rate [FDR] ≤ 0.1, $\log_2$ fold change [FC] ≥ 1) (Fig. 1B; Tables S1 and S2).

As noted above, the transcriptomes from TINs contained transcripts classically associated with immune cells (24). Such transcripts were not observed in PNCs (Fig. S2), except for *Cd80* and *Cd44,* which are receptors that are expressed during

neuron development (28, 29). Thus, the pathways identified in the PNC data that are also identified in the LCM data likely represent neuron-specific responses to *T. gondii*. Functional enrichment analysis of both sample types revealed 975 upregulated pathways shared between infected PNCs and neurons captured *in vivo* (Fig. 2A). A comparison of the top 50 enriched pathways of each condition (LCM or PNCs) identified 14 pathways in common (Table S3). These pathways were associated with responses to different microbial stimuli (e.g., LPS, COVID, and respiratory syncytial virus) and cytokine signaling. By analyzing the individual genes associated with these pathways, we identified a small group of genes that were consistently enriched in these 14 pathways. These genes included CXC motif chemokine ligand 10 (*Cxcl10*, 12 of the 14 pathways), chemokine (C-X-C motif) ligand 1 (*Cxcl1*, 10 of the 14), and chemokine (C-C motif) ligand 2 (*Ccl2*, 9 of the 14) (Fig. 2B). These pathways were functionally similar in that they primarily centered around chemokine/cytokine signaling and proinflammatory responses (Fig. 2C). While both PNCs and the LCM data showed an enrichment of these pathways, the LCM data set showed a higher number of genes involved (set size) and increased $\log_2$FC of the DEGs (Fig. 2C). Only *Ifih1*, *Plaur*, and *Tnfaip3* were highly represented genes that were equivalent or higher in PNCs vs LCM neurons.

A comparison of the downregulated pathways between LCM and PNCs found 28 pathways in common (Fig. 2D). Many of these pathways were neuron-specific, including neuronal markers, protein-protein interactions at synapses (e.g., SNARE proteins), long-term potentiation, activation of NMDA receptors, and GABA synthesis and receptor signaling. We had previously noticed fewer neuron markers in our LCM data set but could not determine if this decrease was due to an increase in contaminating immune cells comprising a higher proportion of our transcripts or a true decrease in neuronal transcription. However, in the PNCs—which lack immune cells—we still saw a decrease in these neuron-specific pathways and related genes (Table S4). In addition to synaptic and neuron marker pathways, multiple voltage-gated potassium channels were downregulated (Fig. 2E). Using the genes from the GO pathway GOMF_POTASSIUM_ION_LEAK_CHANNEL_ACTIVITY, we found that many were downregulated in both of our data sets (Fig. S3) except for Kcnk5/TASK-2, which was upregulated in both paradigms. In summary, the ability to compare the *in vivo* and *in vitro* data sets appears to be a feasible way to identify neuron-specific responses from complex *in vivo* transcriptional studies and suggests that *T. gondii* may directly modulate neuronal function.

Comparison of neuronal responses to *T. gondii* or viral infection

To determine if these neuron responses were specific to *T. gondii* or occurred with other relevant infections, we wanted to compare the LCM and PNC data sets with transcriptional studies from neurons infected with non-parasitic microbes. A search of the Gene Expression Omnibus (GEO) repository, the NIH's publicly funded genomics data repository, identified several transcriptional studies on infected wild-type murine neurons (7, 30–32). From these studies, we analyzed four data sets: Zika virus- and West Nile virus-infected PNCs profiled by microarray (7) and two single-cell RNA-seq studies of cortical neurons infected with a circuit tracing, attenuated rabies virus (31, 32). The latter two data sets (31, 32) had very few genes that met our criteria for DEGs (FDR ≤ 0.1, $\log_2$FC ≥ 1) and were excluded from further analysis. However, the data sets for ZKV and WNV (7) contained 193 and 690 DEGs, respectively (Fig. 3A), making them amenable for comparison with the *T. gondii* data sets.

Between these data sets, there were 532 pathways in common (Fig. 3B). We further narrowed our focus to pathways relating to IFN-γ, IFN-α/β, and TNF signaling to see if there were differences in these responses between infections (Fig. 3C). We found that all data sets had an enrichment for the IFN-γ signaling pathway and innate immunity pathways (represented by Toll-like receptor cascades) (Fig. 3C), but only the viral data sets showed enrichment for TNF signaling. As expected, the viral data sets showed an enrichment in anti-viral, type I IFN pathways, specifically in IFN-stimulated genes. Consistent with prior work (33), *T. gondii*-infected PNCs showed very little type I IFN

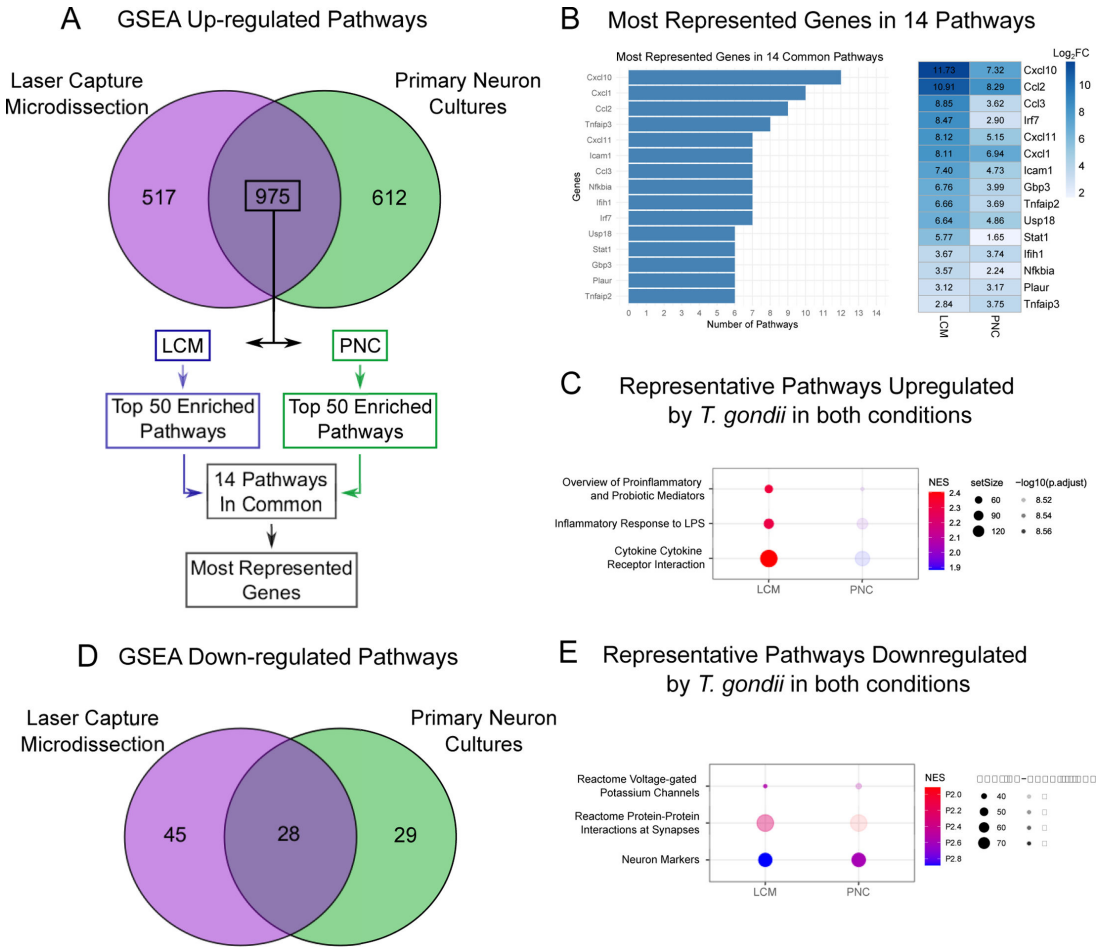

FIG 2 Pathway analysis reveals the neuronal response to *T. gondii* infection involves an increase in proinflammatory cytokines and a decrease in neuron function. (A) The top 14 enriched pathways between LCM data set and PNCs were selected out of 975 upregulated pathways. (B) Quantification of the most represented genes in the 14 most enriched pathways with a heatmap of their log_2FC. (C) Representative signature pathways between PNCs and LCM with normalized enrichment scores (NES). (D) Venn diagram of 28 downregulated pathways in LCM and PNC data sets. (E) Enrichment scores of downregulated neuron pathways in *T. gondii* data sets. GSEA, gene set enrichment analysis.

response, while the LCM data set showed some enrichment in the "Antiviral Mechanism by IFN-Related Antiviral Mechanisms" pathway (Fig. 3C; Fig. S4). To understand these differences, we compared the individual genes involved in type I IFN pathways and found that several key IFN-α genes were differentially expressed (Fig. 3D and E). *T. gondii* PNCs showed upregulation in *Stat1* and *Irf7* but not in many downstream genes. These downstream genes fell into two clusters, with the first cluster (e.g., *Oas2*, *Oas1l*, and *Epsti1*) showing no baseline expression or upregulation and the second cluster (e.g., *Ifnar2* and *Stat2*) showing low baseline expression and no upregulation (Fig. 3E). WNV, ZKV, and, to a lesser extent, *in vivo* infection with *T. gondii* showed the upregulation of many of the genes in this pathway, though differences could be seen even between these three experimental conditions (e.g., *Ifna2, 4, 5, 12*) (Fig. 3D). Collectively, these data suggest that *in vitro*, WNV and ZKV trigger neuron IFN-α responses, but *T. gondii* does not, while *T. gondii* triggers a broader immune response *in vivo*.

DISCUSSION

Here, we sought to define how neurons respond to *T. gondii* and determine how this response compares to infection with other neurotropic microbes. To accomplish this goal, we compared four transcriptional data sets: *T. gondii*-injected neurons captured by

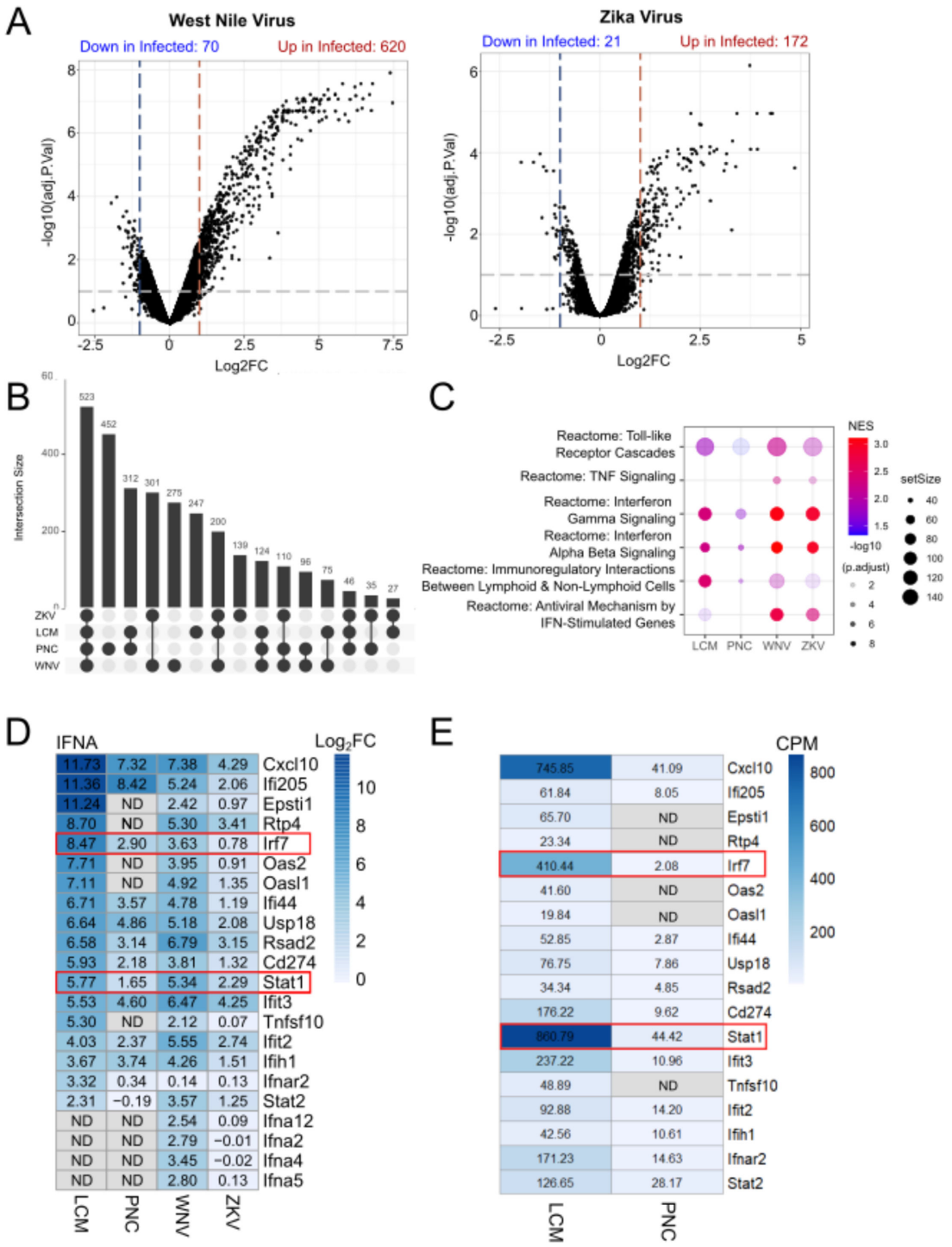

FIG 3 WNV- and ZKV-infected PNCs and the LCM data set show the upregulation of IFN-*α* response genes, unlike *T. gondii*-infected PNCs. (A) Volcano plots of WNV and ZKV-infected PNCs. Horizontal bars indicate adjusted *P* values ≤ 0.1, and vertical bars indicate log2 fold change ≥ 1 for up- and downregulated genes. (B) Upset plot of upregulated gene set enrichment analysis pathways. (C) Relative expression of inflammatory pathways across data sets. (D) IFN-α response genes expressed in LCM, *T. gondii*, WNV, and ZKV infected in log_2FC. (E) Count per million of IFN-α response genes in LCM and *T. gondii* PNC data sets with raw values shown. ND, not detected. ND genes in both LCM and PNCs in panel D are not included in panel E.

LCM from infected murine brain tissue and primary murine cortical neuron cultures infected with *T. gondii*, WNV, or ZKV. These comparisons revealed that cortical neurons

have conserved responses to these infections but also show key differences that distinguish responses to a virus vs a eukaryotic parasite.

All four data sets had a pronounced increase in inflammatory pathways, including in type I and type II interferon signaling (Fig. 3C). Of the many cytokines/chemokines upregulated in these data sets, *Cxcl10* is highly represented in the pathways upregulated in the LCM and *T. gondii*-infected PNC data sets and is also upregulated in WNV- and ZKV-infected PNCs (Fig. 4). These data suggest that *Cxcl10* upregulation is a conserved feature of the neuron response to these infections. As *Cxcl10* is a chemokine that attracts innate and adaptive immune cells, its conserved upregulation is consistent with the need to attract immune cells to infected neurons, whether the infecting microbe is viral or parasitic (e.g., effector T cells for *T. gondii* [34]). Validating the role of neuronal *Cxcl10* and other key genes/pathways in the outcomes of CNS infection will be the focus of future work.

The differences between the data sets are also revealing. Only the *T. gondii* infection data sets showed a consistent downregulation of neuronal function pathways (markers, long term potentiation [LTP], synapse function, and potassium channels). The downregulation in potassium channels was of particular interest to us because it could explain our recent finding that TINs have a depolarized resting membrane potential when compared to non-injected neighboring neurons or neurons in uninfected mice (35). Neuronal dysfunction associated with *T. gondii* infection has been identified previously (36–41), but the experimental setups made it a challenge to distinguish the direct effect of *T. gondii* on neurons vs effects from infiltrating immune cells or microglia and astrocytes. The findings presented here suggest that *T. gondii* can directly induce neuronal dysfunction.

Another interesting example of infection-dependent effects is IFN-α signaling. Akin to other type I IFN responses, IFN-α signaling begins with activation of a host cell pattern recognition receptor (PRR) by a pathogen. This activation leads to IRF7 phosphorylation, resulting in the upregulation of IFN-α. Once released, IFN-α binds to the interferon-α/β receptor (IFNAR), which allows IFN-α to act in an autocrine and paracrine fashion. IFNAR activation leads to the phosphorylation of STAT1 and STAT2, mediating the transcriptional upregulation of a specific set of downstream IFN-α response genes (42) (Fig. 5). As expected, the virus-infected PNCs showed upregulation in genes throughout this pathway, but the two *T. gondii* data sets were less consistent. Both *T. gondii* data sets showed an upregulation in IRF-7 but no upregulation of type I IFNs (α or β) (Fig. S4C). These findings are consistent with prior work in human fibroblasts that suggest that *T. gondii*-infected cells block type I IFN responses (33) upstream of the *T. gondii* effector TgIST, which prevents IFN signaling by binding to pSTAT1/2 heterodimers and pSTAT1 homodimers (43, 44) (Fig. 5). That the *in vivo T. gondii* data set shows the upregulation of some of the downstream IFN response genes suggests that autocrine and paracrine signaling from neuronal and non-neuronal cells may overcome this inhibition *in vivo,* or these downstream genes are upregulated by other pathways. Collectively, these findings are consistent with a model in which neuronal responses to infection depend on the context, with conserved responses arising from pathogen sensors that converge on the same downstream pathways. Such sensors could detect microbes directly or through neuronal stress that, in turn, triggers cellular responses associated with pathogen recognition (45).

MATERIALS AND METHODS

Parasite maintenance

As previously described, type II *T. gondii* (Pruginaud) used in this study was maintained through serial passage in human foreskin fibroblasts (gift of John Boothroyd, Stanford

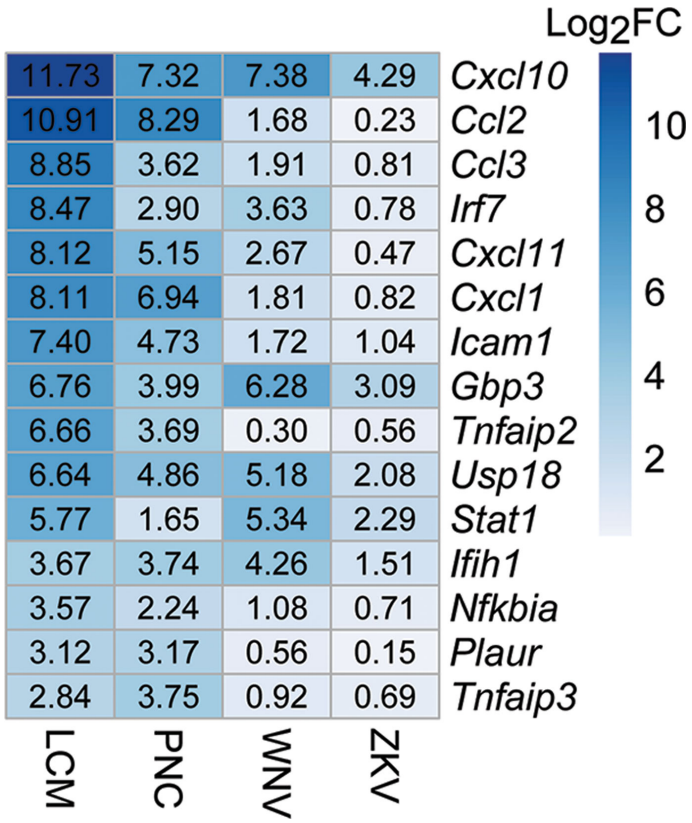

FIG 4 *Cxcl10* is upregulated across acute and subacute data sets. Other conserved genes include *Irf7*, *Icam1*, *Gbp3*, *Usp18*, *Stat1*, and *Ifih1*.

University, Stanford, CA) using Dulbecco's modified Eagle medium (DMEM), supplemented with 10% fetal bovine serum (FBS), 2 mM glutagro, and 100 IU/mL penicillin and 100 µg/mL streptomycin (27).

Mice

All mice were bred and housed in specific-pathogen-free University of Arizona Animal Care facilities. Cre reporter mice (ZsG mice) (mouse stock no. #007906) were originally purchased from Jackson Laboratories.

Primary murine neuron culturing

Mouse primary cortical neurons were harvested from E174 mouse embryos obtained from pregnant ZsG mice. Dissections of E174 cortical neurons were performed, and primary neuronal cell cultures were generated by methods described previously with minor modifications (46). The culturing plates were prepared by coating overnight with 0.001% poly-L-lysine solution (Millipore Sigma, P4707, diluted in water 1:10) for plastic surfaces and 100 µg/mL poly-L-lysine hydrobromide (Sigma, P6282, dissolved in borate buffer, pH 8.4) for glass surfaces. They were washed three times for 10 minutes each with water and transferred to plating media (modified Eagle medium [MEM], 0.6% D-glucose, 10% FBS). Neurons were seeded at 500,000 in 6-well plates for RNA-seq. Four hours after plating, a full media exchange to neurobasal media (Neurobasal base media, 2% B27 supplement, 1% L-glutamine, and 1% penicillin-streptomycin) was performed. On day *in vitro* (DIV) 4, neurons received a half volume media change of neurobasal media with 5 µM cytosine arabinoside (AraC; Millipore Sigma, C6645) to stop glial proliferation. One-third media exchange with neurobasal media occurred every 3–4 days thereafter. All the experiments were performed on 10 DIV neurons.

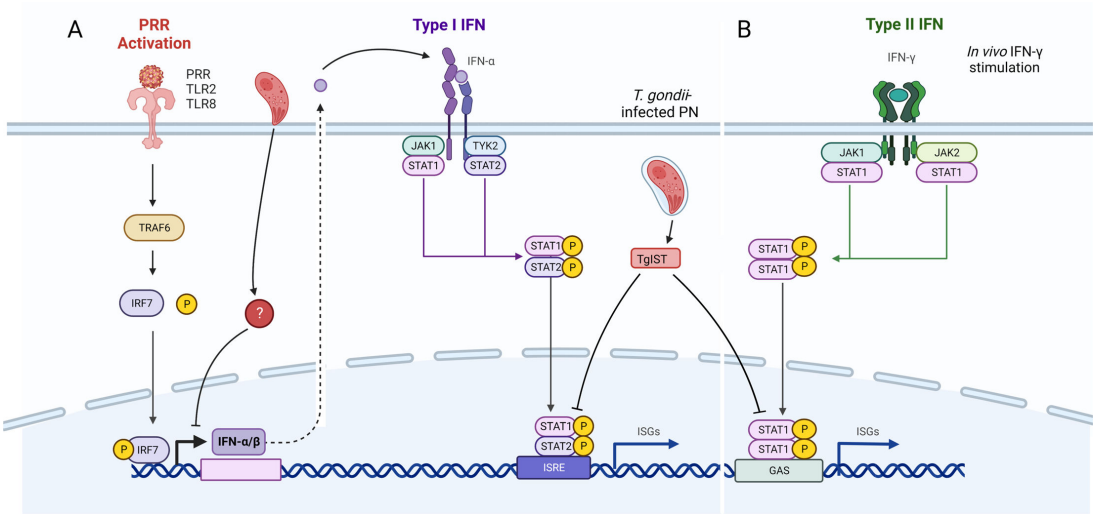

FIG 5 Despite *Irf7* upregulation in all data sets, *T. gondii*-infected neurons fail to upregulate and secrete IFN-α. (A) WNV and *T. gondii* activate PRR receptors leading to an intracellular cascade that results in IFN-α production through IRF7 phosphorylation. IFN-α binds IFNAR and upregulates *Stat1* and other subsequent IFN-α response genes in WNV-infected neurons. *T. gondii* inhibits *Stat1* in this pathway *in vitro* with the *T. gondii* effector protein TgIST. The lack of *Ifn-α* upregulation in both *T. gondii* data sets indicates that the parasite may inhibit the action of phosphorylated IRF7 through an unknown mechanism, either before full invasion or after. (B) *In vivo, Stat1* may be upregulated through alternative stimulation pathways, such as IFN-γ. ISRE = interferon-stimulated response element, GAS = gamma interferon activation site.

RNA isolation, preparation of cDNA libraries, and sequencing

Primary neuronal cell cultures were infected (MOI 5) for 24 hours prior to RNA isolation. Total RNA was extracted using the Direct-zol RNA Miniprep Kit and protocol (Zymo Research, R2051). Samples were sent to Novogene for quality control, library preparation, and sequencing. RNA quality was measured on an Agilent 2100. Only samples with an RNA integrity score of >7 were used. After the QC procedures, mRNA from eukaryotic organisms is enriched using oligo(dT) beads. For prokaryotic or eukaryotic organisms' long non-coding libraries, rRNA is removed using the Ribo-Zero Kit. First, the mRNA is fragmented randomly by adding fragmentation buffer; then, the cDNA is synthesized by using mRNA template and random hexamers primer, after which a custom second-strand synthesis buffer (Illumina), dNTPs, RNase H, and DNA polymerase I are added to initiate the second-strand synthesis. Second, after a series of terminal repair, a ligation, and sequencing adaptor ligation, the double-stranded cDNA library is completed through size selection and PCR enrichment. Paired-end sequencing was performed on an Illumina NovaSeq 6000 at 20 million reads per sample. Initial QC and adapter trimming were performed by Novogene.

RNA-seq analysis and data visualization

Analyses and visualizations were conducted as previously described (47) using a combination of statistical computing environment R version 3, RStudio version 1.2.5042, Bioconductor version 3.1 (48), and Prism 9.4.1 per a previously published training tool (49). Transcript-level counts were summarized to genes using the TxImport package (50) and mouse gene annotation package from biomaRt (51). Data were filtered and normalized with the EdgeR package (52) by the trimmed mean of *M*-values method. Genes with less than one count per million in *n* of the samples (three for PNCs and five for LCM) were filtered out. The VOOM function in Limma (53) was used to variance stabilize the filtered, normalized data. Differential gene expression analysis was performed with Benjamini-Hochberg correction with Limma (53). Gene set enrichment analysis (GSEA) was done using the GSEA software (Broad Institute, version 4.0.2) (54) in R with the GSEABase package. Venn diagrams were generated

with the Venn Diagram tool from VIB/UGent Bioinformatics & Evolutionary Genomics at http://bioinformatics.psb.ugent.be/webtools/Venn/. Heatmaps were generated in R with pheatmap. Microarray data from BioProject PRJNA503843 (7), GSE122121, WNV samples GSM3455732, GSM3455733, and GSM3455734, ZKV samples GSM3455735, GSM3455736, and GSM3455737, and saline samples GSM3455737, GSM3455730, and GSM3455731 were retrieved from the GEO with the GEOquery package. The rabies data set was retrieved in the same manner, GSE38975, samples GSM953148, GSM953149, GSM953150, and GSM953151. Microarray data were analyzed with code from NCBI's GEO2R with the Limma (53) and umap (55) packages.

ACKNOWLEDGMENTS

The authors disclose receipt of the following financial support for the research, authorship, and/or publication of this article: funding by the NIH (R01 AI157247 [A.A.K, C.A.H, D.P.B]); the BIO5 Institute, University of Arizona (A.A.K.). The funders had no role in the study design; data collection, analysis, or interpretation; or the decision to submit the work for publication.

AUTHOR AFFILIATIONS

[1]Neuroscience Graduate Interdisciplinary Program, University of Arizona, Tucson, Arizona, USA
[2]BIO5 Institute, University of Arizona, Tucson, Arizona, USA
[3]Department of Immunobiology, University of Arizona, Tucson, Arizona, USA
[4]Department of Pathobiology, School of Veterinary Medicine, University of Pennsylvania, Philadelphia, Pennsylvania, USA
[5]Department of Neurology, University of Arizona, Tucson, Arizona, USA

AUTHOR ORCIDs

Hannah J. Johnson http://orcid.org/0000-0001-5942-9483
Christopher A. Hunter http://orcid.org/0000-0003-3092-1428
Daniel P. Beiting http://orcid.org/0000-0002-2865-4589
Anita A. Koshy http://orcid.org/0000-0001-8705-3233

FUNDING

Funder	Grant(s)	Author(s)
National Institutes of Health	R01 AI157247	Christopher A. Hunter
		Daniel P. Beiting
		Anita A. Koshy

AUTHOR CONTRIBUTIONS

Hannah J. Johnson, Conceptualization, Data curation, Formal analysis, Investigation, Methodology, Validation, Visualization, Writing – original draft, Writing – review and editing | Joshua A. Kochanowsky, Conceptualization, Investigation, Methodology, Writing – review and editing | Sambamurthy Chandrasekaran, Investigation, Methodology, Writing – review and editing | Christopher A. Hunter, Funding acquisition, Writing – review and editing | Daniel P. Beiting, Conceptualization, Data curation, Formal analysis, Methodology, Resources, Software, Supervision, Writing – review and editing | Anita A. Koshy, Conceptualization, Funding acquisition, Writing – review and editing

DATA AVAILABILITY

The data discussed in this publication have been deposited in NCBI's Gene Expression Omnibus (56, 57) and are accessible through GEO Series accession number GSE293449.

ETHICS APPROVAL

All procedures and experiments were carried out in accordance with the Public Health Service Policy on Human Care and Use of Laboratory Animals and approved by the University of Arizona's Institutional Animal Care and Use Committee (#12-391).

ADDITIONAL FILES

The following material is available online.

Supplemental Material

Supplemental Figures (mSphere00216-25-s0001.pdf). Figures S1 to S4.
Table S1 (mSphere00216-25-s0002.xlsx). DEGs in LCM data set.
Table S2 (mSphere00216-25-s0003.xlsx). DEGs in PNC data set.
Table S3 (mSphere00216-25-s0004.xlsx). Pathways shared between LCM and PNC data sets.
Table S4 (mSphere00216-25-s0005.xlsx). Neuron-associated DEGs in all 4 data sets.

REFERENCES

1. Ferguson DJ, Hutchison WM. 1987. The host-parasite relationship of *Toxoplasma gondii* in the brains of chronically infected mice. Virchows Arch A Pathol Anat Histopathol 411:39–43. https://doi.org/10.1007/BF00734512
2. Garen PD, Tsai TF, Powers JM. 1999. Human eastern equine encephalitis: immunohistochemistry and ultrastructure. Mod Pathol 12:646–652.
3. Colpitts TM, Conway MJ, Montgomery RR, Fikrig E. 2012. West Nile virus: biology, transmission, and human infection. Clin Microbiol Rev 25:635–648. https://doi.org/10.1128/CMR.00045-12
4. Rose RW, Vorobyeva AG, Skipworth JD, Nicolas E, Rall GF. 2007. Altered levels of STAT1 and STAT3 influence the neuronal response to interferon gamma. J Neuroimmunol 192:145–156. https://doi.org/10.1016/j.jneuroim.2007.10.007
5. Cho H, Proll SC, Szretter KJ, Katze MG, Gale M Jr, Diamond MS. 2013. Differential innate immune response programs in neuronal subtypes determine susceptibility to infection in the brain by positive-stranded RNA viruses. Nat Med 19:458–464. https://doi.org/10.1038/nm.3108
6. Daniels BP, Snyder AG, Olsen TM, Orozco S, Oguin TH 3rd, Tait SWG, Martinez J, Gale M Jr, Loo Y-M, Oberst A. 2017. RIPK3 restricts viral pathogenesis via cell death-independent neuroinflammation. Cell 169:301–313. https://doi.org/10.1016/j.cell.2017.03.011
7. Daniels BP, Kofman SB, Smith JR, Norris GT, Snyder AG, Kolb JP, Gao X, Locasale JW, Martinez J, Gale M Jr, Loo Y-M, Oberst A. 2019. The nucleotide sensor ZBP1 and kinase RIPK3 induce the enzyme IRG1 to promote an antiviral metabolic state in neurons. Immunity 50:64–76. https://doi.org/10.1016/j.immuni.2018.11.017
8. Cabral CM, Tuladhar S, Dietrich HK, Nguyen E, MacDonald WR, Trivedi T, Devineni A, Koshy AA. 2016. Neurons are the primary target cell for the brain-tropic intracellular parasite *Toxoplasma gondii*. PLoS Pathog 12:e1005447. https://doi.org/10.1371/journal.ppat.1005447
9. Dubey JP. 2016. Toxoplasmosis of animals and humans. CRC Press.
10. Remington JS, Cavanaugh EN. 1965. Isolation of the encysted form of *Toxoplasma gondii* from human skeletal muscle and brain. N Engl J Med 273:1308–1310. https://doi.org/10.1056/NEJM196512092732404
11. Sullivan WJ, Jeffers V. 2012. Mechanisms of *Toxoplasma gondii* persistence and latency. FEMS Microbiol Rev 36:717–733. https://doi.org/10.1111/j.1574-6976.2011.00305.x
12. Ferguson DJ, Graham DI, Hutchison WM. 1991. Pathological changes in the brains of mice infected with *Toxoplasma gondii*: a histological, immunocytochemical and ultrastructural study. Int J Exp Pathol 72:463–474.
13. Ochiai E, Sa Q, Perkins S, Grigg ME, Suzuki Y. 2016. $CD8^+$ T cells remove cysts of *Toxoplasma gondii* from the brain mostly by recognizing epitopes commonly expressed by or cross-reactive between type II and type III strains of the parasite. Microbes Infect 18:517–522. https://doi.org/10.1016/j.micinf.2016.03.013
14. Salvioni A, Belloy M, Lebourg A, Bassot E, Cantaloube-Ferrieu V, Vasseur V, Blanié S, Liblau RS, Suberbielle E, Robey EA, Blanchard N. 2019. Robust control of a brain-persisting parasite through MHC I presentation by infected neurons. Cell Rep 27:3254–3268. https://doi.org/10.1016/j.celrep.2019.05.051
15. Shallberg LA, Phan AT, Christian DA, Perry JA, Haskins BE, Beiting DP, Harris TH, Koshy AA, Hunter CA. 2022. Impact of secondary TCR engagement on the heterogeneity of pathogen-specific CD8+ T cell response during acute and chronic toxoplasmosis. PLoS Pathog 18:e1010296. https://doi.org/10.1371/journal.ppat.1010296
16. Eberhard JN, Shallberg LA, Winn A, Chandrasekaran S, Giuliano CJ, Merritt EF, Willis E, Konradt C, Christian DA, Aldridge DL, Bunkofske ME, Jacquet M, Dzierszinski F, Katifori E, Lourido S, Koshy AA, Hunter CA. 2025. Immune targeting and host-protective effects of the latent stage of *Toxoplasma gondii*. Nat Microbiol 10:992–1005. https://doi.org/10.1038/s41564-025-01967-z
17. Chandrasekaran S, Kochanowsky JA, Merritt EF, Lagas JS, Swannigan A, Koshy AA. 2022. IFN-γ stimulated murine and human neurons mount anti-parasitic defenses against the intracellular parasite *Toxoplasma gondii*. Nat Commun 13:4605. https://doi.org/10.1038/s41467-022-32225-z
18. Rastogi S, Xue Y, Quake SR, Boothroyd JC. 2020. Differential impacts on host transcription by ROP and GRA effectors from the intracellular parasite *Toxoplasma gondii*. mBio 11:e00182-20. https://doi.org/10.1128/mBio.00182-20
19. Chen L, Christian DA, Kochanowsky JA, Phan AT, Clark JT, Wang S, Berry C, Oh J, Chen X, Roos DS, Beiting DP, Koshy AA, Hunter CA. 2020. The *Toxoplasma gondii* virulence factor ROP16 acts in cis and trans, and suppresses T cell responses. J Exp Med 217:e20181757. https://doi.org/10.1084/jem.20181757
20. Jensen KDC, Wang Y, Wojno EDT, Shastri AJ, Hu K, Cornel L, Boedec E, Ong Y-C, Chien Y, Hunter CA, Boothroyd JC, Saeij JPJ. 2011. *Toxoplasma* polymorphic effectors determine macrophage polarization and intestinal inflammation. Cell Host Microbe 9:472–483. https://doi.org/10.1016/j.chom.2011.04.015
21. Butcher BA, Fox BA, Rommereim LM, Kim SG, Maurer KJ, Yarovinsky F, Herbert DR, Bzik DJ, Denkers EY. 2011. *Toxoplasma gondii* rhoptry kinase ROP16 activates STAT3 and STAT6 resulting in cytokine inhibition and arginase-1-dependent growth control. PLoS Pathog 7:e1002236. https://doi.org/10.1371/journal.ppat.1002236
22. Kochanowsky JA, Thomas KK, Koshy AA. 2021. ROP16-mediated activation of STAT6 suppresses host cell reactive oxygen species production, facilitating type III *Toxoplasma gondii* growth and survival. mBio 12:e03305-20. https://doi.org/10.1128/mBio.03305-20
23. Kochanowsky JA, Chandrasekaran S, Sanchez JR, Thomas KK, Koshy AA. 2023. ROP16-mediated activation of STAT6 enhances cyst development of type III *Toxoplasma gondii* in neurons. PLoS Pathog 19:e1011347. https://doi.org/10.1371/journal.ppat.1011347
24. Merritt EF, Johnson HJ, Wong ZS, Buntzman AS, Conklin AC, Cabral CM, Romanoski CE, Boyle JP, Koshy AA. 2020. Transcriptional profiling suggests T cells cluster around neurons injected with *Toxoplasma gondii*

proteins. mSphere 5:e00538-20. https://doi.org/10.1128/mSphere.00538-20
25. Koshy AA, Fouts AE, Lodoen MB, Alkan O, Blau HM, Boothroyd JC. 2010. *Toxoplasma* secreting Cre recombinase for analysis of host-parasite interactions. Nat Methods 7:307–309. https://doi.org/10.1038/nmeth.1438
26. Madisen L, Zwingman TA, Sunkin SM, Oh SW, Zariwala HA, Gu H, Ng LL, Palmiter RD, Hawrylycz MJ, Jones AR, Lein ES, Zeng H. 2010. A robust and high-throughput Cre reporting and characterization system for the whole mouse brain. Nat Neurosci 13:133–140. https://doi.org/10.1038/nn.2467
27. Koshy AA, Dietrich HK, Christian DA, Melehani JH, Shastri AJ, Hunter CA, Boothroyd JC. 2012. *Toxoplasma* co-opts host cells it does not invade. PLoS Pathog 8:e1002825. https://doi.org/10.1371/journal.ppat.1002825
28. Imitola J, Comabella M, Chandraker AK, Dangond F, Sayegh MH, Snyder EY, Khoury SJ. 2004. Neural stem/progenitor cells express costimulatory molecules that are differentially regulated by inflammatory and apoptotic stimuli. Am J Pathol 164:1615–1625. https://doi.org/10.1016/S0002-9440(10)63720-0
29. Naruse M, Shibasaki K, Yokoyama S, Kurachi M, Ishizaki Y. 2013. Dynamic changes of CD44 expression from progenitors to subpopulations of astrocytes and neurons in developing cerebellum. PLoS One 8:e53109. https://doi.org/10.1371/journal.pone.0053109
30. Gomme EA, Wirblich C, Addya S, Rall GF, Schnell MJ. 2012. Immune clearance of attenuated rabies virus results in neuronal survival with altered gene expression. PLoS Pathog 8:e1002971. https://doi.org/10.1371/journal.ppat.1002971
31. Huang KW, Sabatini BL. 2020. Single-cell analysis of neuroinflammatory responses following intracranial injection of G-deleted rabies viruses. Front Cell Neurosci 14:65. https://doi.org/10.3389/fncel.2020.00065
32. Patiño M, Lagos WN, Patne NS, Tasic B, Zeng H, Callaway EM. 2022. Single-cell transcriptomic classification of rabies-infected cortical neurons. Proc Natl Acad Sci USA 119:e2203677119. https://doi.org/10.1073/pnas.2203677119
33. Beiting DP, Peixoto L, Akopyants NS, Beverley SM, Wherry EJ, Christian DA, Hunter CA, Brodsky IE, Roos DS. 2014. Differential induction of TLR3-dependent innate immune signaling by closely related parasite species. PLoS One 9:e88398. https://doi.org/10.1371/journal.pone.0088398
34. Harris TH, Banigan EJ, Christian DA, Konradt C, Tait Wojno ED, Norose K, Wilson EH, John B, Weninger W, Luster AD, Liu AJ, Hunter CA. 2012. Generalized Lévy walks and the role of chemokines in migration of effector CD8+ T cells. Nature 486:545–548. https://doi.org/10.1038/nature11098
35. Mendez OA, Flores Machado E, Lu J, Koshy AA. 2021. Injection with *Toxoplasma gondii* protein affects neuron health and survival. Elife 10:e67681. https://doi.org/10.7554/eLife.67681
36. Parlog A, Harsan L-A, Zagrebelsky M, Weller M, von Elverfeldt D, Mawrin C, Korte M, Dunay IR. 2014. Chronic murine toxoplasmosis is defined by subtle changes in neuronal connectivity. Dis Model Mech 7:459–469. https://doi.org/10.1242/dmm.014183
37. Brooks JM, Carrillo GL, Su J, Lindsay DS, Fox MA, Blader IJ. 2015. *Toxoplasma gondii* infections alter GABAergic synapses and signaling in the central nervous system. mBio 6:e01428-15. https://doi.org/10.1128/mBio.01428-15
38. Mouveaux T, Roger E, Gueye A, Eysert F, Huot L, Grenier-Boley B, Lambert J-C, Gissot M. 2021. Primary brain cell infection by *Toxoplasma gondii* reveals the extent and dynamics of parasite differentiation and its impact on neuron biology. Open Biol 11:210053. https://doi.org/10.1098/rsob.210053
39. Lang D, Schott BH, van Ham M, Morton L, Kulikovskaja L, Herrera-Molina R, Pielot R, Klawonn F, Montag D, Jänsch L, Gundelfinger ED, Smalla KH, Dunay IR. 2018. Chronic *Toxoplasma* infection is associated with distinct alterations in the synaptic protein composition. J Neuroinflammation 15:216. https://doi.org/10.1186/s12974-018-1242-1
40. David CN, Frias ES, Szu JI, Vieira PA, Hubbard JA, Lovelace J, Michael M, Worth D, McGovern KE, Ethell IM, Stanley BG, Korzus E, Fiacco TA, Binder DK, Wilson EH. 2016. GLT-1-dependent disruption of CNS glutamate homeostasis and neuronal function by the protozoan parasite *Toxoplasma gondii*. PLoS Pathog 12:e1005643. https://doi.org/10.1371/journal.ppat.1005643
41. Haroon F, Händel U, Angenstein F, Goldschmidt J, Kreutzmann P, Lison H, Fischer K-D, Scheich H, Wetzel W, Schlüter D, Budinger E. 2012. *Toxoplasma gondii* actively inhibits neuronal function in chronically infected mice. PLoS One 7:e35516. https://doi.org/10.1371/journal.pone.0035516
42. Delhaye S, Paul S, Blakqori G, Minet M, Weber F, Staeheli P, Michiels T. 2006. Neurons produce type I interferon during viral encephalitis. Proc Natl Acad Sci USA 103:7835–7840. https://doi.org/10.1073/pnas.0602460103
43. Matta SK, Olias P, Huang Z, Wang Q, Park E, Yokoyama WM, Sibley LD. 2019. *Toxoplasma gondii* effector TgIST blocks type I interferon signaling to promote infection. Proc Natl Acad Sci USA 116:17480–17491. https://doi.org/10.1073/pnas.1904637116
44. Olias P, Etheridge RD, Zhang Y, Holtzman MJ, Sibley LD. 2016. *Toxoplasma* effector recruits the Mi-2/NuRD complex to repress STAT1 transcription and block IFN-γ-dependent gene expression. Cell Host Microbe 20:72–82. https://doi.org/10.1016/j.chom.2016.06.006
45. Lopes Fischer N, Naseer N, Shin S, Brodsky IE. 2020. Effector-triggered immunity and pathogen sensing in metazoans. Nat Microbiol 5:14–26. https://doi.org/10.1038/s41564-019-0623-2
46. Parker SS, Moutal A, Cai S, Chandrasekaran S, Roman MR, Koshy AA, Khanna R, Zinsmaier KE, Mouneimne G. 2018. High fidelity cryopreservation and recovery of primary rodent cortical neurons. eNeuro 5:ENEURO.0135-18.2018. https://doi.org/10.1523/ENEURO.0135-18.2018
47. Farias Amorim C, O. Novais F, Nguyen BT, Nascimento MT, Lago J, Lago AS, Carvalho LP, Beiting DP, Scott P. 2021. Localized skin inflammation during cutaneous leishmaniasis drives a chronic, systemic IFN-γ signature. PLOS Negl Trop Dis 15:e0009321. https://doi.org/10.1371/journal.pntd.0009321
48. Huber W, Carey VJ, Gentleman R, Anders S, Carlson M, Carvalho BS, Bravo HC, Davis S, Gatto L, Girke T, et al. 2015. Orchestrating high-throughput genomic analysis with bioconductor. Nat Methods 12:115–121. https://doi.org/10.1038/nmeth.3252
49. Berry ASF, Farias Amorim C, Berry CL, Syrett CM, English ED, Beiting DP. 2021. An open-source toolkit to expand bioinformatics training in infectious diseases. mBio 12:e01214-21. https://doi.org/10.1128/mBio.01214-21
50. Soneson C, Love MI, Robinson MD. 2016. Differential analyses for RNA-seq: transcript-level estimates improve gene-level inferences. F1000Res 4:1521. https://doi.org/10.12688/f1000research.7563.2
51. Durinck S, Spellman PT, Birney E, Huber W. 2009. Mapping identifiers for the integration of genomic datasets with the R/Bioconductor package biomaRt. Nat Protoc 4:1184–1191. https://doi.org/10.1038/nprot.2009.97
52. Robinson MD, McCarthy DJ, Smyth GK. 2010. edgeR: a bioconductor package for differential expression analysis of digital gene expression data. Bioinformatics 26:139–140. https://doi.org/10.1093/bioinformatics/btp616
53. Ritchie ME, Phipson B, Wu D, Hu Y, Law CW, Shi W, Smyth GK. 2015. limma powers differential expression analyses for RNA-sequencing and microarray studies. Nucleic Acids Res 43:e47. https://doi.org/10.1093/nar/gkv007
54. Subramanian A, Tamayo P, Mootha VK, Mukherjee S, Ebert BL, Gillette MA, Paulovich A, Pomeroy SL, Golub TR, Lander ES, Mesirov JP. 2005. Gene set enrichment analysis: a knowledge-based approach for interpreting genome-wide expression profiles. Proc Natl Acad Sci USA 102:15545–15550. https://doi.org/10.1073/pnas.0506580102
55. McInnes L, Healy J, Melville J. 2020. UMAP: uniform manifold approximation and projection for dimension reduction. arXiv. https://doi.org/10.48550/arXiv.1802.03426
56. Edgar R, Domrachev M, Lash AE. 2002. Gene Expression Omnibus: NCBI gene expression and hybridization array data repository. Nucleic Acids Res 30:207–210. https://doi.org/10.1093/nar/30.1.207
57. Barrett T, Wilhite SE, Ledoux P, Evangelista C, Kim IF, Tomashevsky M, Marshall KA, Phillippy KH, Sherman PM, Holko M, Yefanov A, Lee H, Zhang N, Robertson CL, Serova N, Davis S, Soboleva A. 2013. NCBI GEO: archive for functional genomics data sets--update. Nucleic Acids Res 41:D991–D995. https://doi.org/10.1093/nar/gks1193